Supplementary Material

Alginate@$ZnCO_2O_4$ for efficient peroxymonosulfate activation towards efficient Rhodamine B degradation: Optimization using response surface methodology

Badr-Eddine Channab [a], Mohamed EL ouardi [b, c], Salah Eddine Marrane [a], Omar Ait Layachi [d], Ayoub El Idrissi [a], Salaheddine FARSAD [e], Driss Mazkad [f], Amal BaQais[g] Mohammed Lasri [h], Hassan Ait ahsaine[b]

[a] Laboratory of Materials, Catalysis & Natural Resources Valorization, URAC 24, Faculty of Science and Technology, Hassan II University, B.P. 146, Casablanca, Morocco.

[b] Laboratory of Applied Materials Chemistry, Faculty of Sciences, Mohammed V University in Rabat, Morocco

[c] Aix Marseille University, University of Toulon, CNRS, IM2NP, CS 60584, CEDEX 9, F-83041 Toulon, France

[d] Laboratory of physical chemistry and biotechnology of biomolecules and materials, University Hassan II, 20000, Casablanca, Morocco

[e] Materials and Environment Laboratory, Ibn Zohr University, Agadir, 8000, Morocco

[f] Laboratory of Spectroscopy, Molecular Modeling, Materials, Nanomaterials, Water and Environment, Materials for Environment Team, ENSAM, Mohammed V University in Rabat, Morocco

[g] Department of Chemistry, College of Science, Princess Nourah Bint Abdulrahman University, P.O. Box 84428, Riyadh 11671, Saudi Arabia.

[h] Laboratoire of applied chemistry and biomass, departement of chemistry, university cadi ayyad facutly of sciences semlalia BP 2390 marrakech morroco.

Table S1. Experimental range and levels in the BBD for RhB degradation.

Factors	Levels		
	Low (-1)	**Center (0)**	**High (+1)**
X_1: catalyst dose (g)	1	1.5	2
X_2: PMS dose (g)	1	1.5	2
X_3: RhB concentration (mg/L)	20	30	40
X_4: Time (min)	20	30	40

Table S2. Structural parameters of ZCO determined from XRD

Index of plan	**Peak position (2theta)**	**FWHM**	**d-spacing (A)**	**Lattice constant a (A)**	**Cell volume (nm^3)**	**Crystallite size D(nm)**
(111)	19,01	0,237	4,664	8,079	528,425	33,886
(022)	31,29	0,333	2,855	8,076	526,845	24,712
(131)	36,87	0,336	2,435	8,078	527,205	24,865
(222)	38,57	0,277	2,331	8,077	527,038	30,383
(040)	44,84	0,374	2,019	8,077	527,119	22,970
(242)	55,68	0,412	1,649	8,079	527,499	21,776
(151)	59,38	0,468	1,555	8,080	527,554	19,506
(044)	65,27	0,491	1,428	8,079	527,512	19,213

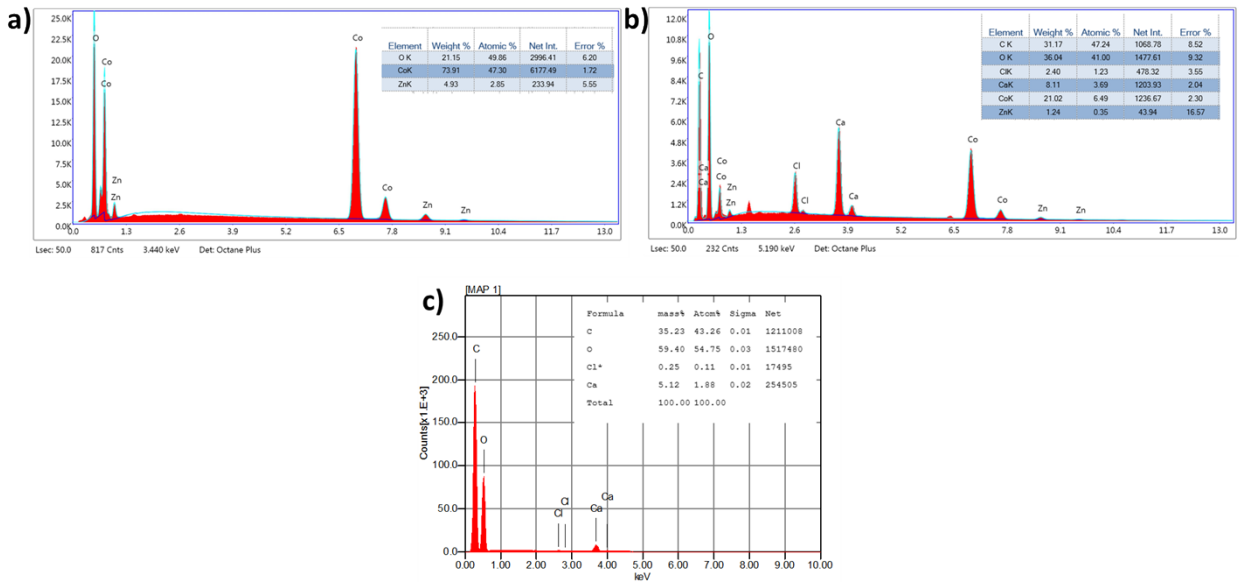

Fig.S1 EDS analysis of ZCO powder **(a)**, ZCO beads **(b)** and Alginate beads **(c)**

1.Thermal analysis

The thermal stability was investigated using thermogravimetric analysis of synthesized materials. The TGA and DTG thermograms of NaAlg, $ZnCo_2O_4$, and NaAlg/$ZnCo_2O_4$ are presented in **Fig. S2**. According to the $ZnCo_2O_4$ thermogravimetric analysis, the material maintains its weight even when heated to 600 °C. the TGA curves of NaAlg indicated three distinct stages of decomposition. The first stage of weight loss was initiated at 58,39°C and increases to 239.26 °C with a percentage weight loss of 23,65 %, with two stages of loss of water molecules related to the various interactions between the polysaccharide and water. The first one, at 96,21 °C, as a result of the loss of free water molecules (6,53%). The loss of more closely coupled water molecules due to polar interactions with carboxylate groups is attributed to the second one at 211,47 °C (17,12%) [1,2]. The second stage of decomposition in the range of 242,78 to 335,10 °C, with a maximum decomposition rate at 283.24°C, accounting for 24,40% of total decomposition, was attributed to the major polymer decomposition step (depolymerization). The final stage of decomposition begins at 406°C (6,13%) due to the degradation of the intermediate composition. It is very evident that NaAlg and NaAlg/$ZnCo_2O_4$ beads exhibit similar degradation characteristics. However, the addition of $ZnCo_2O_4$ nanoparticles improves the thermal stability of the alginate beads. Commonly, the presence of organic and inorganic materials on the surface of nanocomposites can significantly

affect their thermal degradation. In fact, in our study the interactions of $ZnCo_2O_4$ nanoparticles (Zn and Co) with the functional groups on the alginate biopolymer chains (COOH, COO- and OH) (more cross-linking points) which leads to more stable complexes and consequently improved thermal stability of the biocomposite [3].

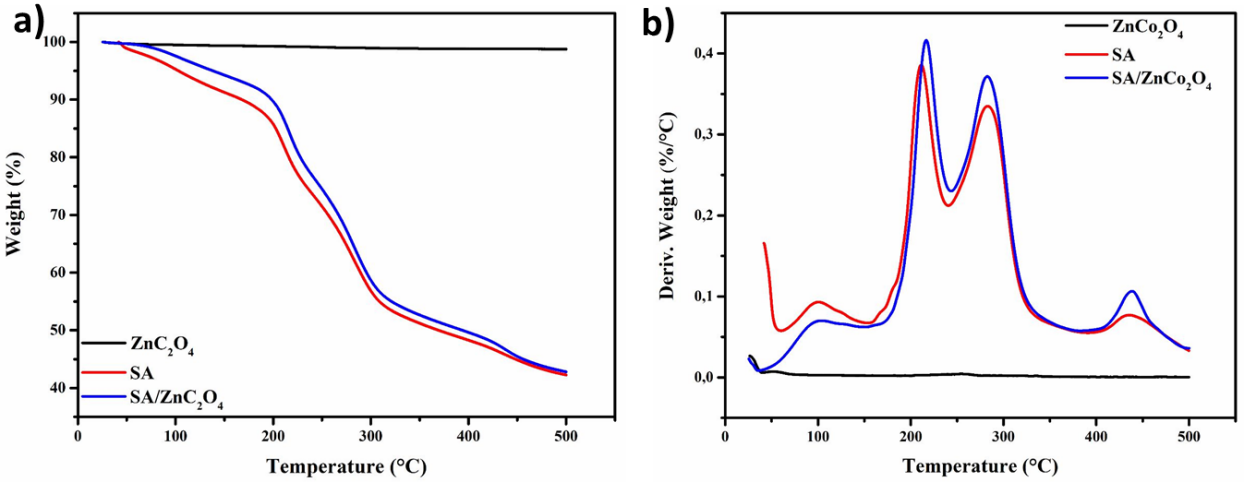

Fig. S2 a, b TGA and DTG of $ZnCo_2O_4$ based materials

2. Stability of beads in pH

The chemical composition and swelling media have a significant impact on the swelling behavior of hydrogel beads. To study the sensitivity of the beads to pH, the swelling behavior of SA and $SA/ZnCo_2O_4$ beads in aqueous solutions of various pH values (1-13) were investigated. The results are presented in **Fig. S3**. As could be observed, the swelling of hydrogel beads containing $ZnCo_2O_4$ was less than that of pure beads. (sodium alginate). The swelling capacity is reduced as a result of the interactions of $ZnCo_2O_4$ nanoparticles with the functional groups on the sodium alginate, which result in more cross-linking points. We can also notice that the equilibrium water uptake of both beads increased with the pH increase from 1 to 5, the equilibrium swelling increases significantly up to become approximately constant in the pH interval of 5 to 9. Afterward, the swelling capacity of both beads decreased gradually in pH range 5 up to 12. The maximum water absorption capacity of both hydrogels has been reached at pH 7.

These obvious changes in the absorption capacity with different pH range may be accounted for as follows.

In an acidic solution, and taking into account the pKa value of the carboxylate groups of sodium alginate (~3.2) [4], the majority of the carboxylate groups ($-COO^-$) were protonated from ($-COO^-$) to (-COOH). In such conditions, the hydrogen bonding interactions betwen the carboxylic acid groups are strongly enhanced. These strong interactions generate further cross-linking points (physical cross-links), which inhibit the polymer–water interactions. Therefore, the beads' swelling rate is relatively reduced. When the pH increases (5<pH<9), When the pH increases (5<pH<9), as a result of the decrease of the H-bonding interaction between the -COOH groups as a result of the dissociation of the carboxylic acid groups (from -COOH to $-COO^-$) it leads to the strengthening of the anion-anion repulsions between the carboxylate groups, and consequently the increase of the swelling capacity [5,6]. Conclusively, these results show that our bio-composite is stable over a wide pH range, a fact that makes it a suitable material for the treatment of urban wastewater identifiable by its almost neutral pH.

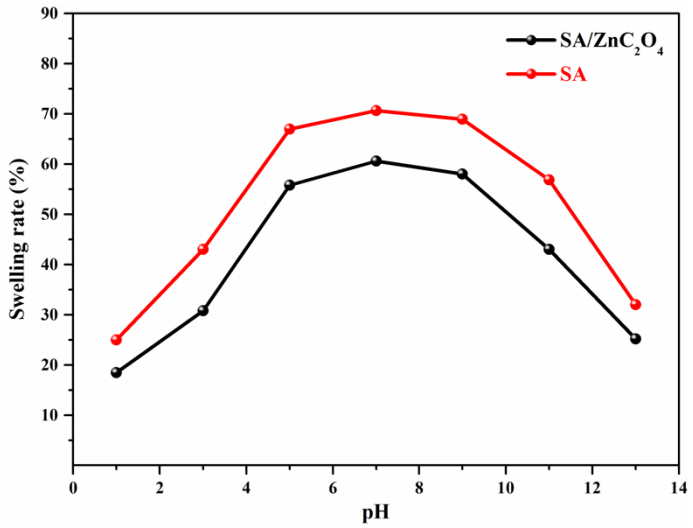

Fig. S3 Swelling behaviors of the prepared beads in various pH.

3. Leaching test

Determining whether the NaAlg@$ZnCo_2O_4$ catalyst operates through a homogeneous or heterogeneous mechanism is crucial. This is because the presence of leached Zn^{2+} and Co^{2+} ions could potentially contribute to the activation of homogeneous PMS (Peroxydisulfate) reactions. To assess the levels of Zn and Co leaching into the NaAlg@$ZnCo_2O_4$/PMS solution during degradation cycles, an inductively coupled plasma (ICP) spectrometer equipped with an AES detector (Ultima2 Jobin Yvon) was used for measurement. Fig. S4(a) illustrates the concentration

of dissolved Co and Zn in the solution derived from the solid catalyst, which exhibits an increasing trend with longer contact time. After 10 minutes, the measured leaching concentrations of Co and Zn are 0.06 mg/L and 0.11 mg/L, respectively. These concentrations then rise to 0.11 mg/L and 0.19 mg/L after 40 minutes. It is worth noting that these leaching results are lower than those reported in the literature for $ZnCo_2O_4$ alone [7,8].

After the reaction, the catalysts were removed, and the resulting solution was designated as the leaching solution. Next, the leaching experiment was initiated by adding the same amount of PMS to the leaching solution. Fig. S4 (b) illustrates that the catalytic activity of the leaching experiment was significantly lower than that of the control experiment, demonstrating that leached metal ions exhibit limited degradation efficiency. Moreover, the degradation processes took place on the NaAlg/$ZnCo_2O_4$ surface in the presence of PMS.

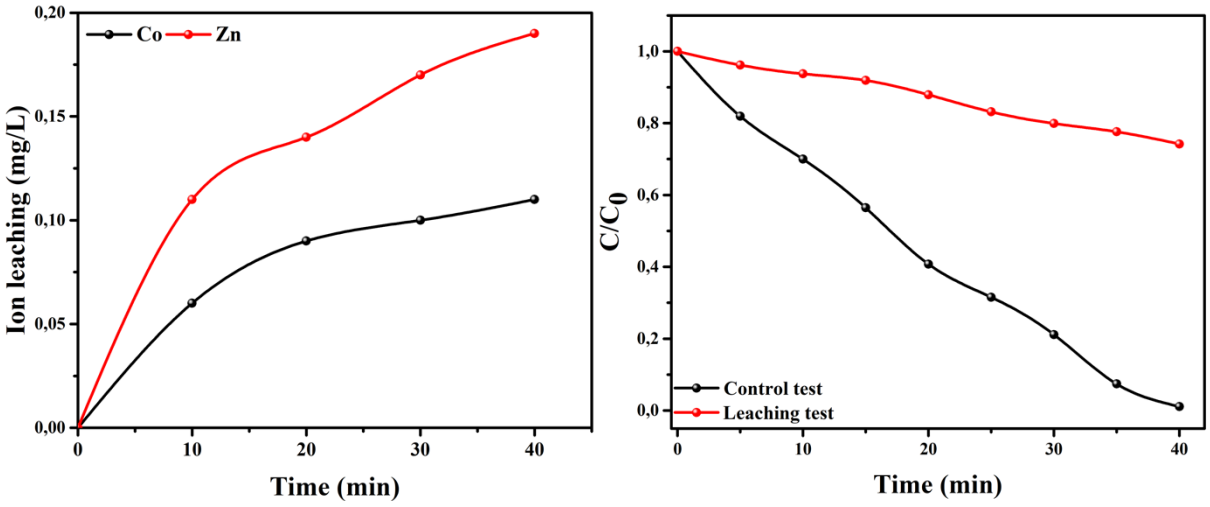

Fig.S4: (a) Concentration of dissolved cobalt and zinc as a function of time (b) The leaching experiment of $ZnCo_2O_4$/PMS system

Table S3. Design matrix for three coded variables together with the actual and predicted responses.

Runs	Coded values of the variables				Responses values (%)	
	X_1	X_2	X_3	X_4	$Y(\%)$	$\hat{Y}(\%)$
1	-1	-1	-1	-1	88,78	89,89
2	1	-1	-1	-1	92,89	92,49
3	-1	1	-1	-1	98,31	97,55
4	1	1	-1	-1	99,97	98,86
5	-1	-1	1	-1	62,21	61,31
6	1	-1	1	-1	66,41	65,55
7	-1	1	1	-1	71,7	71,28
8	1	1	1	-1	73,54	74,22
9	-1	-1	-1	1	96,97	96,39
10	1	-1	-1	1	98,98	98,62
11	-1	1	-1	1	99,98	100,06
12	1	1	-1	1	99,99	100,99
13	-1	-1	1	1	80,08	80,41
14	1	-1	1	1	83,42	84,29
15	-1	1	1	1	85,88	86,38
16	1	1	1	1	90,85	88,96
17	-1	0	0	0	89,73	90,38
18	1	0	0	0	90,9	92,97
19	0	-1	0	0	86,99	87,78
20	0	1	0	0	92,02	93,95
21	0	0	-1	0	99,97	101,00
22	0	0	1	0	79,01	80,70
23	0	0	0	-1	85,75	88,42
24	0	0	0	1	98,99	99,04
25	0	0	0	0	94,87	93,47
26	0	0	0	0	95,32	93,47
27	0	0	0	0	94,03	93,47
28	0	0	0	0	96,76	93,47
29	0	0	0	0	94	93,47
30	0	0	0	0	93,99	93,47

X_1: catalyst mass (g), X_2: PMS mass (g), X_3: RhB concentration (mg/L), X_4: contact time (min), Y is the actual response and $\hat{Y}$ is the predicted response of RhB degradation efficiency (%).

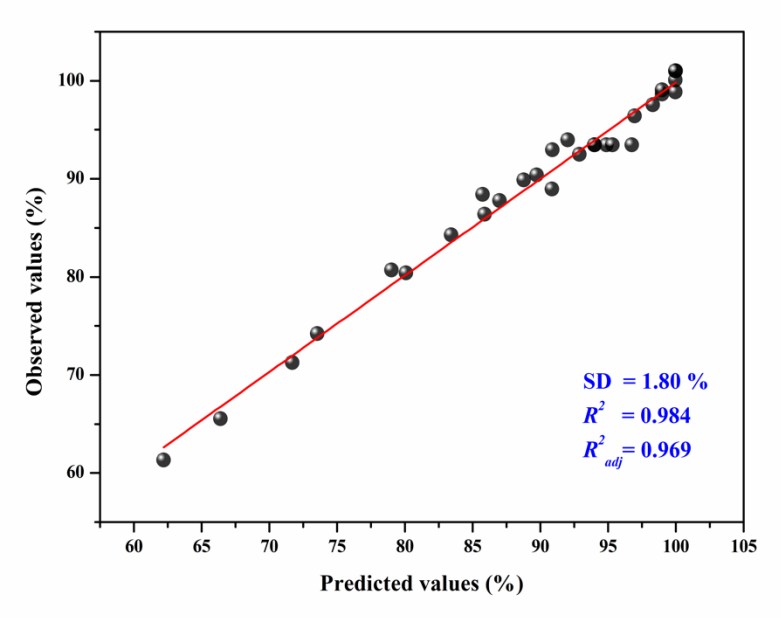

Fig. S5 Graphical plot of predicted Vs actual values of RhB degradation efficiency (%).

Table S4. Analysis of variance (ANOVA) for RhB degradation efficiency (%) using $ZnCo_2O_4$/CaAlg beads

Source	Sum of squares	D_f	Mean square	*F*-Value	*P*-Value (%)	Comments
Regression	3020.73	14	215.767	66.4708	< 0.01 ***	SD = 1.80 %
Residual	48.69	15	3.246	---	---	R^2 = 0.984
Lack of fit	42.689	10	4.268	3.5568	8.7	R^2_{adj} = 0.969
Pure error	6.001	5	1.200	---	---	R^2 = 0.936

Table S5. Estimates and statistics of the coefficients for RhB degradation efficiency (%).

Terms	**Coefficient**	**SE coefficient**	***t*-Value**	***P*-Value %**
Constant	93.470	0.559	167.01	< 0.01 ***
X_1	1.295	0.424	3.05	0.811 **
X_2	3.083	0.424	7.26	< 0.01 ***
X_3	-10.152	0.424	-23.91	< 0.01 ***
X_4	5.310	0.424	12.50	< 0.01 ***
X_1X_1	-1.796	1.119	-1.61	12.9
X_2X_2	-2.606	1.119	-2.33	3.42 *

X_3X_3	-2.621	1.119	-2.34	3.34 *
X_4X_4	0.258	1.119	0.23	82.1
X_1X_2	-0.323	0.450	-0.72	48.3
X_1X_3	0.410	0.450	0.91	37.7
X_2X_3	0.576	0.450	1.28	22.0
X_1X_4	-0.092	0.450	-0.21	84.0
X_2X_4	-0.998	0.450	-2.22	4.25 *
X_3X_4	3.150	0.450	6.99	< 0.01 ***

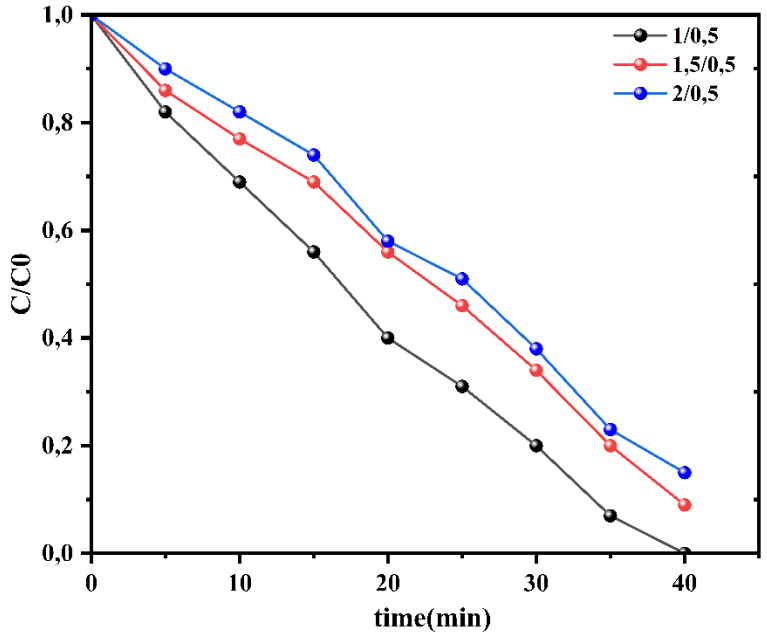

Fig. S6 The influence of the quantity of sodium alginate on the catalytic performance of the catalyst.

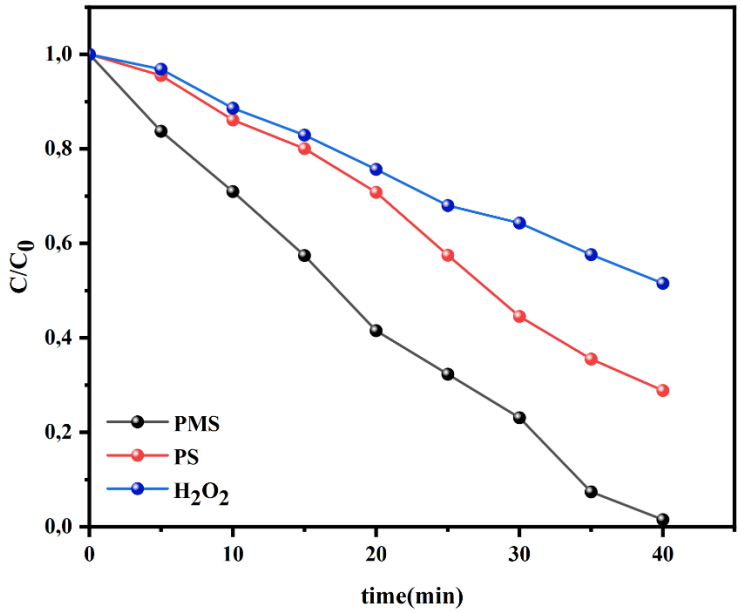

Fig. S7 A comparison of various oxidants upon the decomposition of RhB using ZCO/Alg catalyst. Under the conditions, [Catalyseur] = 1 g/L, [RhB] = 25mg/L, [PMS] = 1 g/L, ambient temperature.

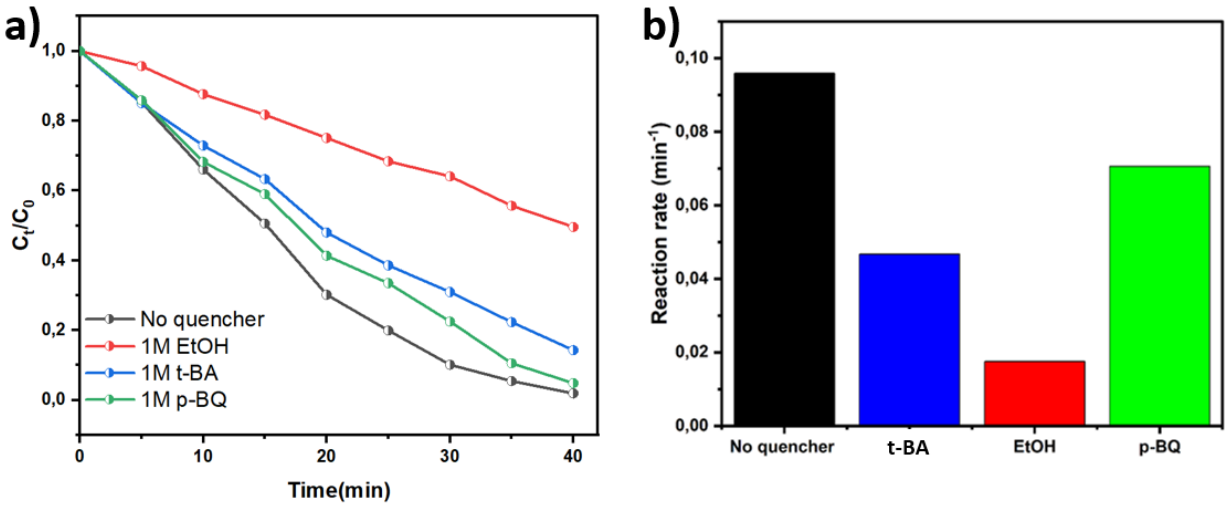

Fig. S8 Radical competition analysis of RhB decomposition. **(a)** Impact of quenching agents of tert-butyl alcohol (t-BA-1M) and ethanol (EtOH-1M) on RhB degradation rate. **(b)** The variation of the reaction rate constant in the presence and the absence of quenching agents. Under the conditions, [Catalyseur] = 1 g/L, [RhB] = 25mg/L, [PMS] = 1 g/L, ambient temperature.

1 L. Nouri, S. Hemidouche, A. Boudjemaa, F. Kaouah, Z. Sadaoui and K. Bachari, *International Journal of Biological Macromolecules*, 2020, **151**, 66–84.
2 P. Laurienzo, M. Malinconico, A. Motta and A. Vicinanza, *Carbohydrate Polymers*, 2005, **62**, 274–282.
3 S. Chkirida, N. Zari, R. Achour, H. Hassoune, A. Lachehab, A. el kacem Qaiss and R. Bouhfid, *Journal of Photochemistry and Photobiology A: Chemistry*, 2021, **412**, 113215.
4 S. Hua, H. Ma, X. Li, H. Yang and A. Wang, *International Journal of Biological Macromolecules*, 2010, **46**, 517–523.
5 B. Rashidzadeh, E. Shokri, G. R. Mahdavinia, R. Moradi, S. Mohamadi-Aghdam and S. Abdi, *International Journal of Biological Macromolecules*, 2020, **154**, 134–141.
6 T. Lu, T. Xiang, X.-L. Huang, C. Li, W.-F. Zhao, Q. Zhang and C.-S. Zhao, *Carbohydrate Polymers*, 2015, **133**, 587–595.
7 L. Hu, G. Zhang, M. Liu, Q. Wang and P. Wang, *Chemosphere*, 2018, **212**, 152–161.
8 Y. Gao and D. Zou, *Chemical Engineering Journal*, 2020, **393**, 124795.